25th ABCM International Congress of Mechanical Engineering
October 20-25, 2019, Uberlândia, MG, Brazil

COB-2019-1729
Aeroelastic Gust Response for the Von Kármán Spectrum Considering a Leading-edge Flap

Natália Sayuri Masunaga
São Paulo State University (UNESP), Dept. of Mechanical Enginering, Ilha Solteira, SP
sayuri.masunaga@unesp.br
Douglas Domingues Bueno
São Paulo State University (UNESP), Dept. of Mathematics, Ilha Solteira, SP
douglas.bueno@unesp.br

Abstract: *This work investigates the spectrum distribution of continuous gust loads found in the atmosphere. It is evaluated the effects of a leading-edge flap coupled to the trailing-edge flap for an aeroelastic system with four degrees of freedom. The control surfaces coupling parameter is investigated to determined the stable and unstable system behavior. The different gust configurations are studied and unsteady aerodynamic forces are considered. The equations of motion are written using aeroelastic frequency response functions (FRF) and the system responses are obtained in terms of their power spectral density (PSD).*

Keywords: *Leading-edge flap, Response spectrum to continuous gust loads, Aeroelastic frequency response function*

1. INTRODUCTION

During development of a new aircraft, stability analyzes and aeroelastic responses are necessary, with requirements that may affect the design, and even restrict the flight envelope. The calculation of gust loads is an important analysis process during aircraft design. The study of aeroelastic phenomena arising from the interaction between fluids and structures is an important area of research called aeroelasticity which makes gust response analysis being an extremely important topic. Gust loads are naturally occurring in the atmosphere and may compromise the airworthiness of structural integrity of air vehicles. It is important to guarantee the system's stability, thus, the structure of an aircraft is economically viable when low structural weight is achieved, which leads to the design of more flexible structures. But increased flexibility can lead to problems of dynamic origin, such as instability, which compromise the integrity of the structure.

Among different design strategies aimed at alleviate continuous gust loads, the use of control surfaces such as ailerons has proved viable, including applications in Boeing, Airbus and Lockheed Martin aircraft. Some of the approaches used include the Lambie (2011) model, which was used to control the propeller bending, relieving the acting nonstationary aerodynamic loads. Wang *et al.* (2012) have been able to suppress aeroelastic vibrations in a nonlinear wing using actuators in the leading and trailing-edge flaps. However, there is a few works exploring the use of leading-edge flap to alleviate gust loads such as studied by Carvalho (2017).

Therefore, in order to improve the airworthiness conditions in turbulent atmosphere, this work evaluates the power spectral density distribution due to the variation of the physical properties of the turbulence. Also, its evaluates the effect on stability and flexibility of a leading-edge flap due a coupling factor relative to the trailing-edge flap at the aeroelastic response spectrum for suppression of continuous gust loads of Von Kármán. It will be considered a typical four degrees of freedom section with nonstationary aerodynamics. The work has relevance to the development of safer aeronautical systems.

2. METHODOLOGY

The system considered has four degrees of freedom, as shown in Fig. 1. Since θ is the rotation of the airfoil relative to the direction of flow, β the trailing-edge flap, γ the leading-edge flap and α the angle between the velocity of the flow and center of gravity. The other variables are defined as: *c.g.* the center of gravity, *e.c.* the elastic center, *a.c.* the aerodynamic center, k_i the springs, b the semi-chord, *TE* the trailing-edge flap and *LE* the leading-edge flap.

The equation of motion of the system is given by Eq. 1. For the purposes of structural analysis, it is considered that there is no damping in the system.

$$\mathbf{M}\ddot{\mathbf{u}}(t) + \mathbf{B}\dot{\mathbf{u}}(t) + \mathbf{K}\mathbf{u}(t) = \mathbf{F}_a + \mathbf{F}_g(\omega) \tag{1}$$

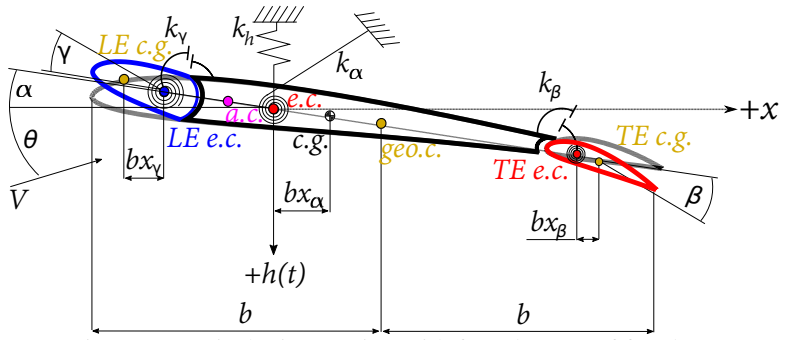

Figure 1: Typical wing section with four degrees of freedom.

The matrices of mass $\mathbf{M}$, damping $\mathbf{B}$ and stiffness $\mathbf{K}$ were presented by Edwards (1977) for a airfoil with four degrees of freedom, which were subsequently coupled using the coupling factor n presented by Lambie (2011), as exposed in Eq. 2 and Eq. 3.

$$\mathbf{M} = mb^2 \begin{bmatrix} 1/b & x_\alpha & x_\gamma - nx_\beta \\ x_\alpha/b & r_\alpha^2 & [x_\gamma(d-a) - r_\gamma^2] - n[r_\beta^2 + x_\beta(c-a)] \\ (x_\beta + nx_\gamma)/b & [r_\beta^2 + x_\beta(c-a)] + n[x_\gamma(d-a) - r_\gamma^2] & nr_\gamma^2 - nr_\beta^2 \end{bmatrix} \tag{2}$$

$$\mathbf{K} = mb^2 \begin{bmatrix} \omega_h^2/b^2 & 0 & 0 \\ 0 & \omega_\theta^2 r_\theta^2 & 0 \\ 0 & 0 & \omega_\gamma^2 r_\gamma^2 \end{bmatrix} \tag{3}$$

In Equation 1, $\mathbf{F}_a = q\mathbf{Q}(s')\mathbf{u}(s')$ represents the unsteady vector of aerodynamic forces of Jaworski (2012) and $\mathbf{F}_g$ is the gust load forces. The aeroelastic system (Eq.1) is rewritten by the array of FRF $\mathbf{H}(\omega)$ in Equation 10, where the superwritings R and I respectively indicate the real and imaginary parts of the matrix and $\eta = 1/m\pi$. The aeroelastic response spectrum $\mathbf{U}(\omega) = \{h(\omega)\ \theta(\omega)\ \beta(\omega)\ \gamma(\omega)\}^T$ (where $h(\omega)$ is the vertical displacement or *plunge* of the airfoil) due to the gust load is obtained from $\mathbf{U}(\omega) = \mathbf{H}(\omega)\mathbf{F}_g(\omega)$. Equation 4 represents the nonstationary aerodynamic matrix $\mathbf{Q}$ for each frequency reduced k which was given by Theodorsen (1935) properly altered Jaworski (2012).

$$\mathbf{Q}(ik) = 2qb^2 \left\{ -\mathbf{M}_{nc}k^2 + [\mathbf{B}_{nc} + C(k)\mathbf{R}\mathbf{S}_2]\, jk + [\mathbf{K}_{nc} + C(k)\mathbf{R}\mathbf{S}_1] \right\} \tag{4}$$

where $q = \frac{1}{2}\rho V^2$ is the dynamic pressure, the sub-index nc represents the noncirculatory terms and $C(k)$ is an approximation of function of Theodorsen. Jaworski (2012) defined the noncirculatory matrices $\mathbf{M}_{nc}$ and $\mathbf{K}_{nc}$, also the vectors $\mathbf{S}_1$, $\mathbf{S}_2$ and $\mathbf{R}$, which were coupled according to Lambie (2011).

$$\mathbf{M}_{nc} = \rho b^4 \begin{bmatrix} \frac{\pi}{b^2} & -\frac{\pi a}{b} & \frac{Z_2}{b} + n\frac{T_1}{b} \\ \frac{\pi a}{b} & -\pi\left(\frac{1}{8} + a^2\right) & -Z_4 + n2T_{13} \\ \frac{T_1}{b} + n\frac{Z_2}{b} & -2T_{13} + nZ_4 & \left[\left(-\frac{Z_{12}}{\pi} - n\frac{T_3}{\pi}\right) + n\left(\frac{Z_8}{\pi} - n\frac{Z_{12}}{\pi}\right)\right] \end{bmatrix} \tag{5}$$

$$\mathbf{K_{nc}} = \rho b^2 U^2 \begin{bmatrix} 0 & 0 & 0 \\ 0 & 0 & -Z_{16} + nT_{15} \\ 0 & 0 & \left[\left(\frac{Z_{18}}{\pi} + n\frac{T_{18}}{\pi}\right) + n\left(-\frac{Z_{23}}{\pi} + n\frac{Z_{21}}{\pi}\right)\right] \end{bmatrix} \tag{6}$$

$$\mathbf{S_1} = \rho b^2 U^2 C \begin{bmatrix} 0 & 1 & \frac{Z_{13}}{\pi} - n\frac{T_{10}}{\pi} \end{bmatrix} \tag{7}$$

$$\mathbf{S_2} = \rho b^3 U C \begin{bmatrix} \frac{1}{b} & \left(\frac{1}{2} - a\right) & \frac{Z_{14}}{2\pi} - n\frac{T_{11}}{2\pi} \end{bmatrix} \tag{8}$$

$$\mathbf{R} = \begin{bmatrix} \frac{2\pi}{b} & 2\pi\left(\frac{1}{2} + a\right) & -T_{12} + nZ_{15} \end{bmatrix}^T \tag{9}$$

$$\mathbf{H}(\omega) = \left[-\omega^2\mathbf{M} + j\omega\mathbf{B} - j(\eta/\mu)0,5\mathbf{Q}^I + \left(\mathbf{K} - (\eta/\mu)0,5\mathbf{Q}^R\right)\right]^{-1} \tag{10}$$

Obtained the FRF, it is necessary to determine an equation that represents the gust load found by an aircraft in flight. According to Karpel (1981), the vertical gust power spectral density of Von Kármán represented by Eq. 11 is used

$$\Phi_{wg}(\Omega) = \frac{\sigma_w^2}{\pi}\frac{L}{V}\frac{1+(8/3)(1.3387L\Omega)^2}{[1+(1.3387L\Omega)^2]^{11/6}} \tag{11}$$

where σ_w the RMS velocity of the gust, Ω the spatial frequency of the excitation given by $\Omega = \omega/V$ and L the scale of the turbulence. Finally, the spectrum of the gust response is obtained by the Transfer Function Theorem, represented in Eq. 12

$$\begin{Bmatrix} \Phi_h(\omega) \\ \Phi_\alpha(\omega) \\ \Phi_{(\beta_{(\omega)}-n\gamma_{(\omega)})} \end{Bmatrix} = \left|\ \mathbf{H}^2\ \right|^2 \begin{Bmatrix} \Phi_{wg}(\omega) \\ 0 \\ 0 \end{Bmatrix} \tag{12}$$

where $|\mathbf{H}|^2 = \mathbf{H}\cdot\mathbf{H}^*$ is a multiplication of a FRF by its conjugate complex and "*n*" is the coupling factor (or parameter). The vertical power spectral density of Von Kármán only acts in movement of *plunge*.

3. RESULTS AND DISCUSSIONS

As specified in MIL-HDBK-1797 (2009), Tab. 1 presents the parameters values assumed to carry out the numerical simulations. The spectrum of gust can be obtained at low frequencies, but from a value above $10^{-3}(m/s)^2/Hz$ to a height of $300m$. In Fig. 2 it is noticed that the increase in the wavelength characteristic of the turbulence results in an increasing linear variation in the spectrum distribution of gust loads resulting a greater amplitude in the initial spectrum $\Phi_{wg}(0)$ and also in the maximum points $\Phi_{wg,max}$. The increase in air velocity results in decay in the initial value of the spectrum and amplitudes of the maximum points such that this variation is more visible at lower velocities where the spectrum distribution of gust loads is on the order of 10^5.

Table 1: Physical parameters of gust loads.

Mean aerodynamic chord	$b = 1\ m$
Air density	$\rho = 1,1638\ kg/m^3$
Air Velocity	$V = 275\ m/s$
Vertical wavelength characteristic of the turbulence	$L_g = 762\ m$
RMS value of turbulent velocity	$\sigma_{wg} = 1\ b/s^2$
Frequency ($\Delta = 0,001\ Hz$)	$0\ Hz \leq f \leq 200\ Hz$

Figure 2: Variation of spectrum distribution of gust loads as a function of physical parameters of the gust loads.

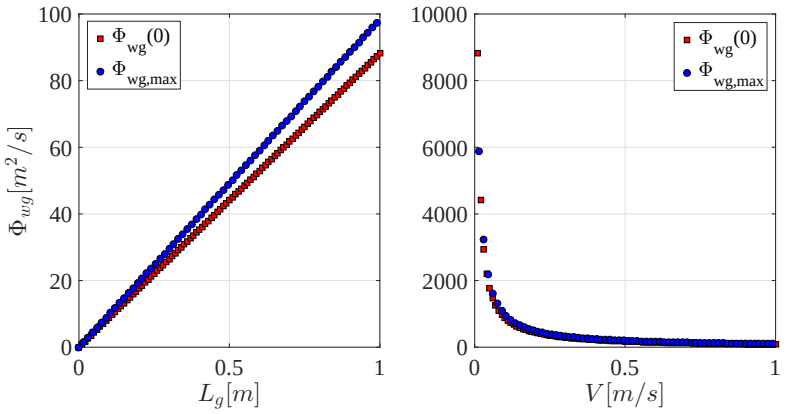

The numerical simulations consider an airfoil defined as Edwards (2013), for which Tab. 2 shows the values of each parameter. The system previously described by four degrees of freedom is redefined by 3 DOFs coupling the leading-edge flap with the trailing-edge flap using the rule $\beta_{(\omega)} = -\eta\gamma_{(\omega)}$. It is evaluated this coupled configuration, in which both flaps rotate simultaneous and synchronized, as discussed by Lambie (2011) and Carvalho (2017). For this case, the system stability is verified because an stable behavior can be achieved depending on the "*n*", as show in Fig. 3. For a coupling factor of $0 \geq n \geq 10$, its concluded that spin radius variation has a value that guarantees stability and a maximum coupling factor to the system of $n = 8$. Also, the natural frequency variation results in a maximum coupling factor around $n = 1.7$ and its not possible to obtain flaps coupled with natural frequencies below $\omega_\gamma = 100 rad/s$.

Table 2: Physical and geometric parameters for a typical wing section with three degrees of freedom coupled.

Natural frequency of h	$\omega_h = 50\ rad/s$
Natural frequency of α	$\omega_\alpha = 100\ rad/s$
Natural frequency of β	$\omega_\beta = 300\ rad/s$
Natural frequency of β	$\omega_\gamma = 500\ rad/s$
Distance of the dimensionless elastic center	$a = -0.4\ m$
Reference semi-chord	$b = 0.5\ m$
Distance of dimensionless control surface	$c = 1\ m$
Dimensionless mass displacement center	$x_\alpha = 0.2$
Dimensionless mass displacement center	$x_\beta = 0.0125$
Dimensionless mass displacement center	$x_\beta = 0.0125$
Spin radius of typical wing section	$r_\alpha = \sqrt{0.25}$
Spin radius of trailing-edge	$r_\beta = \sqrt{0.00625}$
Spin radius of leading-edge	$r_\gamma = \sqrt{0.00625}$
Mass ratio $(m_s/\pi\rho b^2)$	$\mu = 40$

Figure 3: Components of the torsional stiffness of the leading-flap edge k_γ normalized by their maximum values.

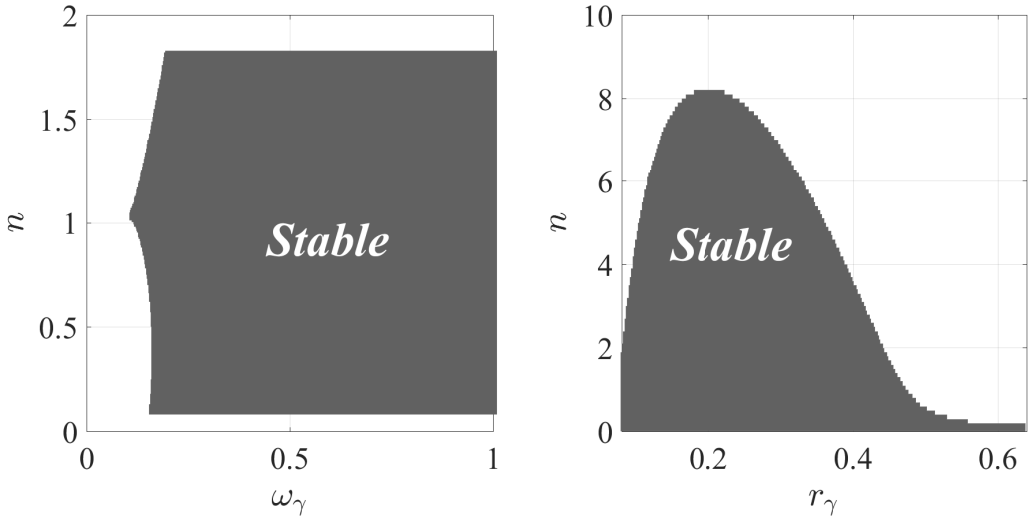

Based on Fig. 3 from Fig. 4 it is observed that the aeroelastic response spectrum for suppression of continuous gust loads of the coupled flaps at lower aeroelastic frequencies as the coupling factor increases. Futhermore, the variation of the coupling factor does not influence the *pitch* and *plunge* movement. But, values of n higher than 3.75 results in instability of the system with flexibility defined in $\omega_\gamma = 500\ (rad/s)$ and $r_\gamma = \sqrt{0.00625}$, once imaginary part of eigenvalues is negative out of stable area.

Fixing the coupling factor with $n = 0.5$, Fig. 5 presents an analysis about the increase in the spin radius and the natural frequency of the leading-edge flap, which results in an alleviation at continuous gust loads as a consequence of the reduction at the aeroelastic response spectrum in vertical displacement of typical wing section (*plunge*) with three degrees of freedom coupled. The term governed by the natural frequency of the leading-edge flap offers a greater alleviation at continuous gust loads because it presents larger numbers high squared.

Figure 4: Aeroelastic response spectrum in the frequency domain in function of coupling factor "n".

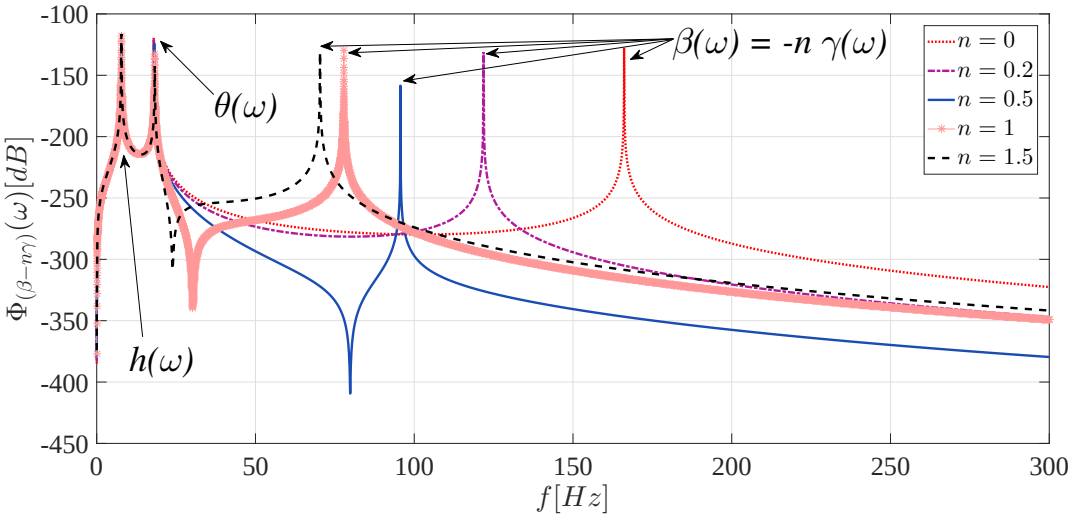

Figure 5: Variation of the aeroelastic response spectrum in $h(\omega)$ in function of the radius of rotation and natural frequency of the leading-edge flap.

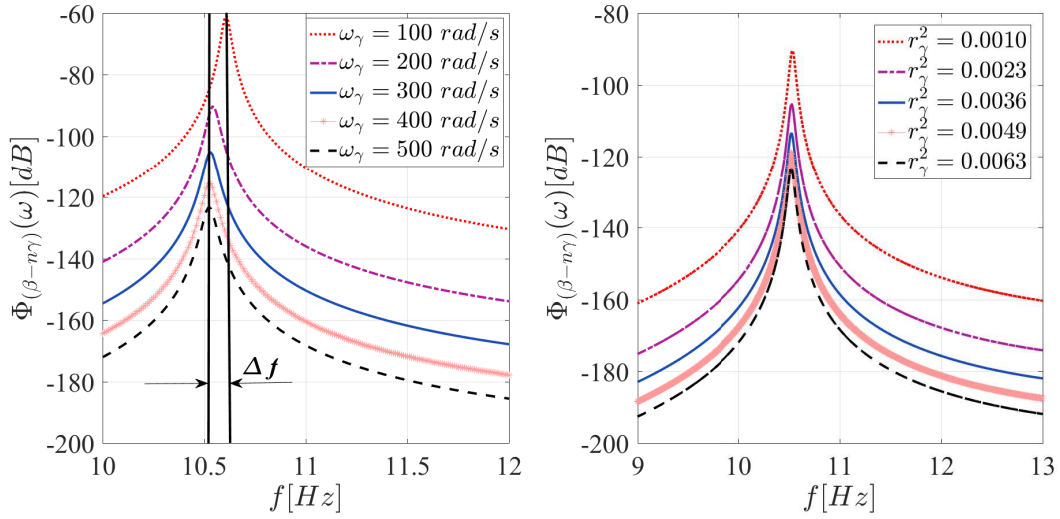

Futhermore, it is noted that the increase in natural frequency, to a value around $500 rad/s$, reduces and advances the magnitude of the response spectrum from $f = 10.61Hz$ to $f = 10.51Hz$ with a frequency variation of $\Delta f = 0.1Hz$, since, from this value, this variation is minimal and can be overlooked. With respect to the spin radius, it has a maximum value which is able to reduce the magnitude of the response spectrum, since it has relation with the rotation of the airfoil and can result in phase inversion and opposite effect when the values that guarantee the stability of the system are not choosed.

4. CONCLUSION

This articles investigated the aeroelastic response spectrum considering continuous gust spectrum. A system with 4 DOFs, containing two control surfaces (on its trailing and lead edges), was rewritten by 3 DOFs by coupling both control surfaces, one in each other. Stable and unstable dynamic behavior were identified for different coupling factors.

The study evaluated the power spectral density of Von Kármán for different values of its physical parameters of the turbulence, and based on the analysis it was possible to associate each configuration with and system spectral responses. The main conclusion is that the increase in the aeroelastic response depends on the higher turbulence characteristic length. Otherwise, the reduction of the responses can be achieved by reducing the free flow velocity.

Finally, it is verified that is possible to alleviate the continuous gust loads by reducing the aeroelastic response spectrum in vertical displacement of a typical wing section with a coupled three degrees of freedom two flaps system, which is obtained by increasing the flexbility of the leading-edge flap to a value that still guarantees the system's stability.

5. ACKNOWLEDGEMENTS

The authors would like to thank CNPq (*Conselho Nacional de Desenvolvimento Científico e Tecnológico*) to sponsor the scholarship through the *Edital* PIBIC 04/2018.

6. REFERENCES

Carvalho, F.I., 2017. *Estudo do Comportamento Aeroelástico de um Sistema Passivo de Supressão de Cargas de Rajada*. Master's thesis, Instituto Tecnológico de Aeronáutica, Campo Montenegro - São José dos Campos - SP -Brasil.

Edwards, J.W., 1977. "Unsteady aerodynamic modeling and active aeroelastic control". Technical Report N78-10017, NASA, Stanford University, California.

Edwards, J., 2013. "Active flutter control using genegeneral unsteady aerodynamic theory". *AIAA Journal*, Vol. 1, No. 1, p. 9.

Jaworski, J.W., 2012. "Thrust and aerodynamic forces from an oscillating leading edge flap". *AIAA Journal - Technical Notes*, Vol. 50, No. 12, pp. 1–4. doi:10.2514/1.J051579.

Karpel, M., 1981. "Desgin for active and passive flutter suppression and gust alleviation". Technical Report GRANT NGL-05-020-243, NASA, Stanford, California.

Lambie, B., 2011. *Aeroelastic Investigation of a Wind Turbine Airfoil with Self-Adaptive Camber*. Ph.D. thesis, Technischen Universitat Darmstadt, Darmstadt, Department of Mechanical Engineering-Fluid Mechanics and Aerodynamics (SLA).

MIL-HDBK-1797, 2009. "Flying qualities of piloted aircraft". Technical report, Department of Defense Interface Standard.

Theodorsen, T., 1935. "General theory of aerodynamic instability and the mechanism of flutter". *NACA Rept. 496*, Vol. 13, pp. 374–387.

Wang, Z., Behal, A. and Marzocca, P., 2012. "Continuous robust control for two-dimensional airfoils with leading and trailing-edge flaps". *Journal of Guidance, Control, and Dynamics*, Vol. 35, No. 2. doi:10.2514/1.54347. University of Central Florida, Orlando, Florida and Clarkson University, Potsdam, New York.

7. RESPONSIBILITY NOTICE

The authors, Natália Sayuri Masunaga and Douglas Domingues Bueno, are solely responsible for the content of this work.